AJNR

Localized Proton MR Spectroscopy of the Allocortex and Isocortex in Healthy Children

Choong-Gon Choi, Tae-Sung Ko, Ho Kyu Lee, Jung Hee Lee and Dae Chul Suh

AJNR Am J Neuroradiol 2000, 21 (7) 1354-1358
http://www.ajnr.org/content/21/7/1354

AJNR Am J Neuroradiol 21:1354–1358, August 2000

Localized Proton MR Spectroscopy of the Allocortex and Isocortex in Healthy Children

Choong-Gon Choi, Tae-Sung Ko, Ho Kyu Lee, Jung Hee Lee, and Dae Chul Suh

BACKGROUND AND PURPOSE: **The human allocortex is different from the isocortex in neuroglial cytoarchitecture. The purpose of this study was to compare metabolic data of the allocortex with those of the isocortex by using localized proton MR spectroscopy.**

METHODS: **Short-TE stimulated-echo acquisition mode proton MR spectroscopy (TR/TE = 3000/30) was applied to the allocortex of the temporal lobe and isocortex of the parietal or frontal lobe in 30 healthy children (19 boys and 11 girls, 3–14 years old). Peak intensities of *N*-acetylaspartate (NAA), choline-containing compounds (Cho), and *myo*-inositol (mI) relative to creatine and phosphocreatine (Cr) were calculated. Metabolic data from the investigated regions were compared.**

RESULTS: **NAA/Cr was significantly lower in the allocortex than in the isocortex of the parietal or frontal lobe: 1.05 ± 0.12 (n = 33) vs. 1.36 ± 0.10 (n = 28) or 1.32 ± 0.10 (n = 12), respectively. Cho/Cr and mI/Cr were significantly higher in the allocortex than in the isocortex: 0.84 ± 0.11 vs. 0.56 ± 0.06 or 0.75 ± 0.10; 0.78 ± 0.15 vs. 0.54 ± 0.08 or 0.66 ± 0.09, respectively. In the isocortex, NAA/Cr was not different but Cho/Cr and mI/Cr were significantly higher in the frontal cortex than in the parietal cortex.**

CONCLUSION: **Clear metabolic differences were observed between the allocortex and isocortex.**

The human cerebral cortex is composed of multiple neuronal cell layers mixed with glial cell components. For over a century, it has been well recognized that cortical neurons are arranged in certain laminar patterns and that the cerebral cortex displays regional differences in these patterns. The cerebral cortex can be divided into the allocortex and the isocortex according to histologic characteristics. The allocortex is so named because it displays a wide variation of histologic patterns in different regions (1). In contrast, the isocortex has a more uniform histologic pattern in different regions. The allocortex is characterized by three neuronal layers—molecular, pyramidal or granular, and polymorphic—and includes the cornu ammonis, dentate gyrus, and parahippocampal gyrus. Most of the parahippocampal gyrus is a transitional zone between the allocortex and isocortex. The isocortex, which comprises most of the cerebral cortex, is also known as the neocortex and is characterized primarily by six neuronal layers (1).

The normal human allocortex, or hippocampal area, has been studied extensively with the use of proton MR spectroscopy, especially in studies of temporal lobe epilepsy, but just to serve as control data (2–5). The characteristics of the normal allocortex, despite its importance, have rarely been studied (6–8) and have not been compared directly with the isocortex. This study was designed to compare metabolic data of the allocortex with those of the isocortex.

Methods

Subjects

During a period of 2 years, 34 children with nonspecific symptoms such as severe headache or dizziness were referred for brain MR imaging/MR spectroscopy from the pediatric neurology department. All patients were examined and determined to be neurologically normal by a pediatric neurologist. Four children with a history of frequent febrile convulsions or difficult delivery were excluded from the pool of subjects owing to the possibility of brain damage. Thus, a total of 30 subjects (19 boys and 11 girls, 3–14 years old; mean age, 9 years) were included in this study. Most of the children were cooperative during the examination, except for a few young children who were sedated with a small amount of oral chloral hydrate (10% syrup, 100 mg/mL) before the examination.

Received August 11, 1999; accepted after revision February 15, 2000.

From the Departments of Radiology (C-G.C., H.K.L., D.C.S.) and Pediatric Neurology (T-S.K.), Asan Medical Center, University of Ulsan College of Medicine; and the Department of Radiological Science, Asan Institute for Life Sciences (J.H.L.), Seoul, Korea.

Address reprint requests to Choong-Gon Choi, MD, Department of Radiology, Asan Medical Center, University of Ulsan, 388-1 PoongNap-Dong, SongPa-Gu, Seoul 138-736, Republic of Korea.

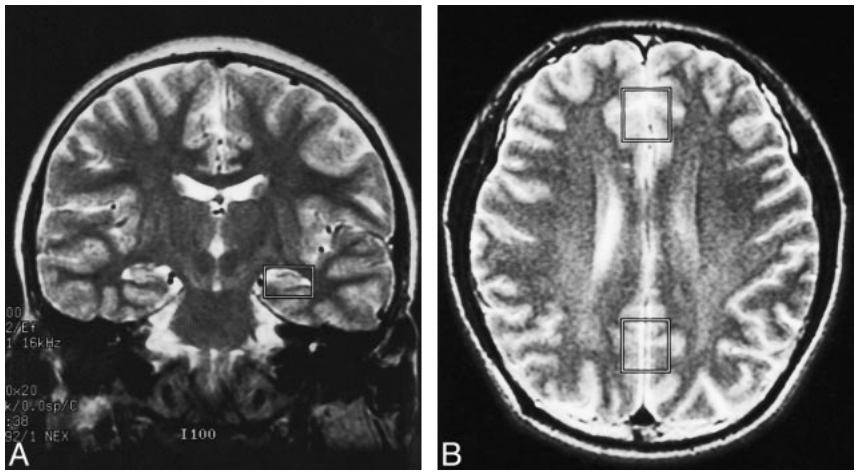

FIG 1. *A* and *B*, Coronal (*A*) and axial (*B*) T2-weighted MR images show typical locations selected for proton MR spectroscopy of the allocortex (*A*), parietal cortex, and frontal cortex (*B*).

Proton MR Spectroscopy

Proton MR spectroscopy was performed on a 1.5-T system using a standard imaging head coil. Patients were positioned using soft pads such that the neck was slightly hyperextended. Thereafter, orthogonal axial and sagittal T1-weighted images and axial and coronal T2-weighted images were obtained according to the following MR imaging protocol: for T1-weighted images, spin-echo sequences were obtained with TR/TE = 500/11, field of view = 200–240 mm, slice thickness = 5 mm with no gap, and matrix = 256 × 192; for T2-weighted images, fast spin-echo sequences were obtained with TR/TE = 3500/102, echo train length = 8, field of view = 200 mm, slice thickness = 5 with no gap, and matrix = 256 × 192.

Automated short-TE proton MR spectra were recorded in the allocortex and isocortex of the frontal or parietal lobe with the use of a single-voxel stimulated-echo acquisition mode sequence (TR/TE/excitations = 3000/30/96, mixing time = 13.7 milliseconds, spectral width = 2500 Hz, number of points = 2048). The voxel size for the allocortex was fitted into the rectangular box shape (14 × 18 × 20 mm, 5 mL), taking both the anatomy of the hippocampus and parahippocampal gyrus and the signal-to-noise ratio into consideration. Special attention was paid to selecting the location of the voxel on coronal T2-weighted localizer images to ensure coverage of the hippocampus and parahippocampal gyrus as much as possible within the volume of interest (Fig 1A). The spectra from the isocortex were obtained with our routine voxel size (18 × 20 × 20 mm, 7.2 mL) (Fig 1B).

Acquired spectroscopic raw data were transferred to a workstation (SPARC 10, Sun Computer, Mountain View, CA) and processed using postprocessing software (SA/GE, Milwaukee, WI). The processing consisted of water-referenced correction of the eddy current effect (9), lorentzian to gaussian transformation, gaussian line broadening of 0.5 Hz, zero-filling of 8K, Fourier transformation, and zero-order phasing of the transformed spectrum. Major peaks at 2.01, 3.03, 3.22, and 3.56 ppm were assigned to *N*-acetylaspartate (NAA), creatine and phosphocreatine (Cr), choline-containing compounds (Cho), and *myo*-inositol (mI), respectively (10). After the measurement of peak areas by lorentzian-gaussian fitting, metabolic ratios (NAA/Cr, Cho/Cr, and mI/Cr) were calculated using Cr as an internal reference, because the reported concentrations of Cr were similar in the various regions of the normal cerebral cortex, including the allocortex (11–13).

In all, 81 spectra were acquired in the 30 subjects, consisting of 40 spectra from bilateral studies of the allocortex in 20 subjects, 29 spectra from the parietal cortex in 29 subjects, and 12 spectra from the frontal cortex in 12 subjects, resulting in 2.7 spectra per subject, on average. All MR imaging and MR spectroscopy studies were usually finished within 1 hour. Eight spectra that contained features of distorted baseline, prominent motion artifacts, or insufficient water suppression were regarded as poor quality. Most of the poor-quality spectra (seven of eight) were obtained from the allocortex, which was expected owing to the large susceptibility differences in this anatomic location. One poor-quality spectrum obtained from the parietal cortex was caused by patient motion during the examination. Seventy-three spectra were included in the final data set, consisting of 33 spectra from the allocortex, 28 from the parietal cortex, and 12 from the frontal cortex.

Statistics

Spectroscopic data were reported as mean ± 1 SD. A one-way ANOVA test was used to examine the difference in mean values among three groups. A two-sided unpaired *t*-test assuming equal variances was used to examine the difference in mean values between two groups (SPSS for Windows, release 7.5). Also, age-dependent changes of metabolic ratios were tested by correlation and linear regression analysis. *P* values less than .05 were considered significant.

Results

The allocortex showed no significant hemispheric asymmetry in metabolic ratios in comparisons of the mean values from the right and left side in 17 subjects (for NAA/Cr: 1.05 ± 0.11 vs. 1.04 ± 0.14, $P = .41$; for Cho/Cr: 0.85 ± 0.10 vs. 0.83 ± 0.13, $P = .24$; for mI/Cr: 0.75 ± 0.12 vs. 0.80 ± 0.18, $P = .24$). Therefore, the average value of both sides of the allocortex is used in the following discussion. Spectroscopic data are summarized in the Table. Figure 2 shows representative short-TE proton MR spectra obtained from the allocortex and isocortex. The allocortex had a lower NAA/Cr ratio and higher Cho/Cr and mI/Cr ratios than did the isocortex. Within the isocortex, NAA/Cr was not different, but Cho/Cr and mI/Cr were significantly higher in the frontal cortex than in the parietal cortex. Spectroscopic data are plotted against age of the children (Fig 3); however, we found no observable tendency for age-dependent changes in metabolic ratios. Similarly, there was no significant correlation between age and metabolic ratios in either the allocortex or isocortex ($P > .05$).

Spectroscopic data from the allocortex and isocortex

	Allocortex (n = 33)	Isocortex: Parietal (n = 28)	Isocortex: Frontal (n = 12)	*P*
NAA/Cr	1.05 ± 0.12	1.36 ± 0.10	1.32 ± 0.10	<.001†
P		<.001	<.001	
		.352*		
Cho/Cr	0.84 ± 0.11	0.56 ± 0.06	0.75 ± 0.10	<.001†
P		<.001	.017	
		<.001*		
mI/Cr	0.78 ± 0.15	0.54 ± 0.08	0.66 ± 0.09	<.001†
P		<.001	.020	
		<.001*		

Note.—Mean values ± 1 SD are given. *P* values are for a two-sided unpaired *t*-test comparison between the allocortex and isocortex.

*Values are for a two-sided unpaired *t*-test comparison within the isocortex.

†Values are for one-way ANOVA test.

Discussion

Because the T1 and T2 relaxation times of major brain metabolites do not show significant regional differences in the cerebral cortex of healthy subjects (8, 14) and because NAA is generally accepted as a neuronal marker (15), the observed lower NAA/Cr in the allocortex may be the result of relatively low NAA concentration in this region. Previous quantitative proton MR spectroscopy studies have also reported relatively low NAA concentrations in the allocortex (2, 8). Compared with the six-layered isocortex, the neuronal component of the allocortex is composed primarily of scattered large pyramidal neurons in the middle layer of the cornu ammonis, small granular neurons in the dentate gyrus, and the neurons within the parahippocampal gyrus, which is a transitional zone between the three-layered allocortex and the six-layered isocortex. A cytoarchitectural study reported lower neuronal density in the allocortex than in the isocortex (16), supporting spectroscopic results.

The relatively high Cho/Cr and mI/Cr ratios in the allocortex may be caused by higher concentrations of Cho and mI than in the isocortex, in agreement with previous quantitative proton MR spectroscopy studies (8, 11). The major Cho metabolites detected by proton MR spectroscopy—phosphorylcholine, glycerophosphorylcholine, and Cho plasmalogen—are involved in the metabolism of membrane Cho phospholipid. Once the active myelination process is completed within 2 years after birth, regional differences in Cho concentrations in the normal brain may depend mainly on the cell density and cell types of the anatomic regions. A proton MR spectroscopy study of cell type-specific cultures revealed Cho concentration to be two or three times higher in glial cells (astrocyte or oligodendrocyte) than in neurons (17). Therefore, we speculate that the higher Cho concentration in the allocortex may be due to relatively high glial density as compared with the isocortex. The allocortex may have relatively larger amounts of glial components, especially in the thick molecular and polymorphic layer of the dentate gyrus and cornu ammonis, which have very low neuronal cell densities.

mI seems to be involved in the osmoregulatory system in astrocytes (18). A multinuclear MR spectroscopy study of cell type-specific cultures suggested that mI is located mainly in astrocytes (19). We therefore speculate that mI concentration may depend on the astrocytic density of the anatomic region in healthy subjects. The relatively high mI/Cr ratio in the allocortex may be the result of its higher astrocytic density than in the isocortex. Our speculation is supported by a study showing the greatest intensity of cortical astrocyte marker (glutamine synthetase) in the allocortex as compared with other regions of the brain in rats (20). However, cytoarchitectural data from the human brain may be necessary to verify this theory.

As far as the isocortex is concerned, there was no significant difference in NAA/Cr between the frontal and parietal cortices. This finding may be

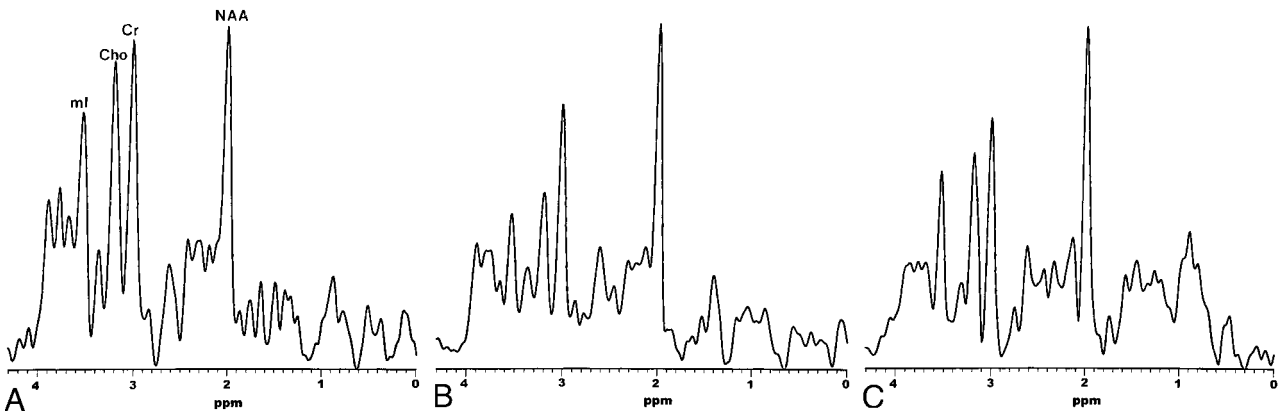

FIG 2. *A–C,* Typical proton MR spectra obtained from the allocortex (*A*), parietal cortex (*B*), and frontal cortex (*C*). Acquisition and processing parameters used for all spectra are the same as described in the text, except for voxel sizes, which are 5.0 mL for the allocortex and 7.2 mL for the isocortex. All spectra are scaled individually and cannot be used for direct comparison. NAA, 2.01 ppm; Cr, 3.03 ppm; Cho, 3.22 ppm; mI, 3.56 ppm.

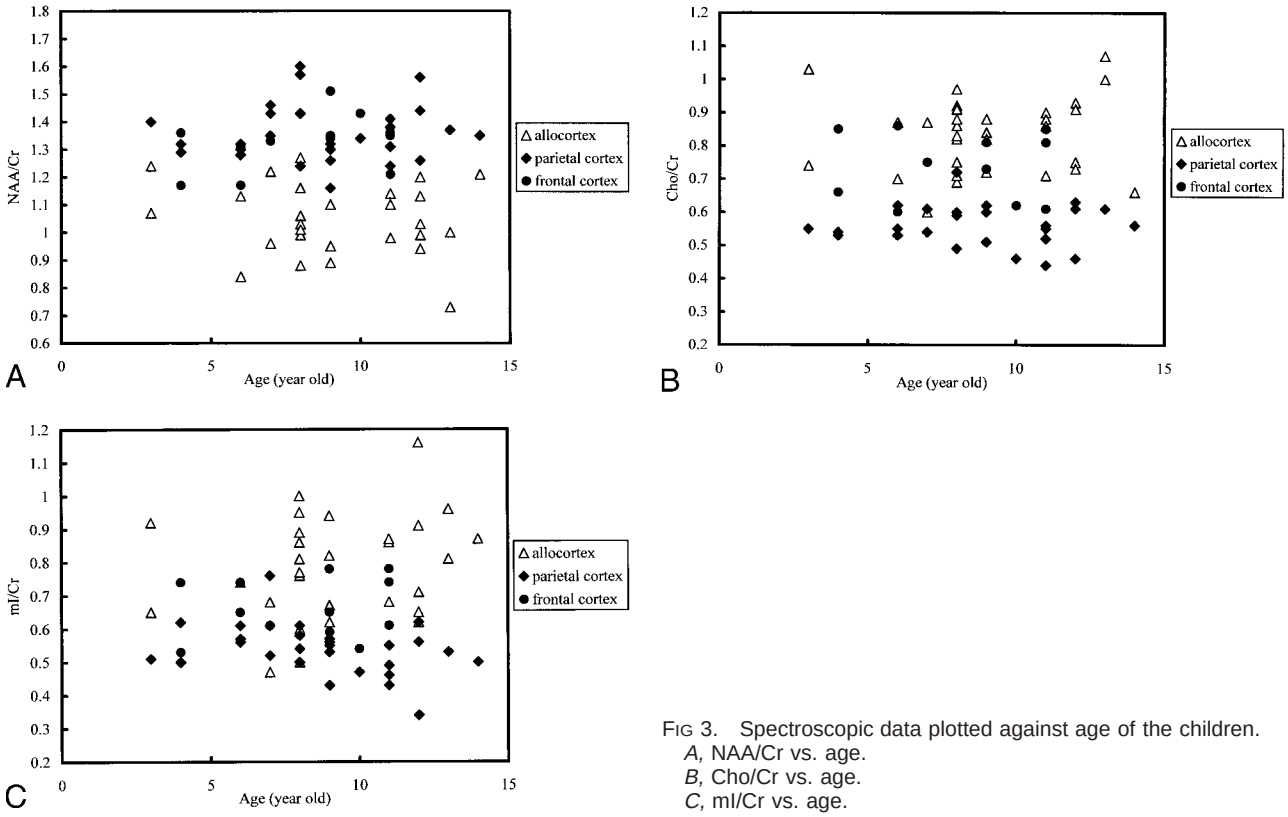

FIG 3. Spectroscopic data plotted against age of the children.
A, NAA/Cr vs. age.
B, Cho/Cr vs. age.
C, mI/Cr vs. age.

due to similar neuronal densities in both regions. von Economo (16) classified the isocortex into five basic types—agranular, frontal, parietal, polar, and atypical granular—on the basis of the cytoarchitectural patterns of the granular and pyramidal neurons. The parietal and frontal isocortex investigated in this study belongs to the same frontal type; therefore, it may have a similar neuronal cytoarchitecture or density, which may account for the observed similar NAA/Cr ratios in both regions. On the other hand, the higher Cho/Cr and mI/Cr seem to be caused by the higher glial density in the frontal cortex. A quantitative proton MR spectroscopy study (11) also detected a higher Cho concentration in the frontal cortex than in the parietal or occipital cortex. Previous cytoarchitectural studies have usually focused on the neuronal composition of the cerebral cortex and have paid little attention to the glial counterpart (1, 16). However, more recently, it has become well recognized that the glial counterpart plays an essential role in the proper functioning of the cortex (21, 22). Neuroglial composition may be different in various regions to adapt to the functions of the cerebral cortices (20, 23, 24).

Because the subjects in our study were all children, age-dependent changes in metabolites should be taken into consideration. A previous quantitative MR spectroscopy study found that Cr and mI concentrations in children's brains become similar to those of adults within 2 years after birth, and that NAA and Cho concentrations continue to change slowly until age 7 years (25). In this study of 3- to 14-year-olds, we detected no age-dependent changes in the various metabolic ratios. It seems that children's brains maintain a stable cellular composition and metabolism once active myelination is completed.

Conclusion

Clear metabolic differences were found between the allocortex and isocortex in the brains of healthy children. As compared with the isocortex, the allocortex is characterized by a relatively low NAA/Cr ratio and high Cho/Cr and mI/Cr ratios. We speculate that these spectroscopic differences may correlate with the regional differences in cortical neuroglial composition; however, further histologic–spectroscopic correlation is needed to support our speculation.

Acknowledgments

We gratefully acknowledge the technical assistance of Sang-Tae Kim and Sun-Woo Lee in patient preparation and data acquisition. We also thank Byung-Hee Min for proofreading the manuscript.

References

1. Clemente CD. **Developmental and gross anatomy of the central nervous system.** In: Clemente CD, ed.*Gray's Anatomy,* 30th American ed. Philadelphia: Lea & Febiger; 1985;1075–1082
2. Breiter SN, Arroyo S, Mathews VP, Lesser RP, Bryan RN, Barker PB. **Proton MR spectroscopy in patients with seizure disorders.** *AJNR Am J Neuroradiol* 1994;15:373–384

3. Ng TC, Comair YG, Xue M, et al. **Temporal lobe epilepsy: presurgical localization with proton chemical shift imaging.** *Radiology* 1994;193:465–472
4. Lu D, Margouleff C, Rubin E, et al. **Temporal lobe epilepsy: correlation of proton magnetic resonance spectroscopy and ^{18}F-fluorodeoxyglucose positron emission tomography.** *Magn Reson Med* 1997;37:18–23
5. Woermann FG, McLean MA, Bartlett PA, Parker GJ, Duncan JS. **Short-echo time single-voxel 1H magnetic resonance spectroscopy in magnetic resonance imaging-negative temporal lobe epilepsy: different biochemical profile compared with hippocampal sclerosis.** *Ann Neurol* 1999;45:369–376
6. Strauss WL, Tsuruda JS, Richards TL. **Partial volume effects in volume-localized phased-array proton spectroscopy of the temporal lobe.** *J Magn Reson Imaging* 1995;4:433–436
7. Bernard D, Walker PM, Baudouin-Poisson N, et al. **Asymmetric metabolic profile in mesial temporal lobes: localized H-1 MR spectroscopy in healthy right-handed and non-right-handed subjects.** *Radiology* 1996;199:381–389
8. Choi CG, Frahm J. **Localized proton MRS of the human hippocampus: metabolite concentrations and relaxation times.** *Magn Reson Med* 1999;41:204–207
9. Klose U. **In vivo proton spectroscopy in presence of eddy currents.** *Magn Reson Med* 1990;14:26–30
10. Michaelis T, Merboldt KD, Haenicke W, Gyngell ML, Bruhn H, Frahm J. **On the identification of cerebral metabolites in localized ^{1}H NMR spectra of human brain in vivo.** *NMR Biomed* 1991;4:90–98
11. Pouwels PJ, Frahm J. **Regional metabolite concentrations in human brain as determined by quantitative localized proton MRS.** *Magn Reson Med* 1998;39:53–60
12. Peeling J, Sutherland G. **^{1}H magnetic resonance spectroscopy of extracts of human epileptic neocortex and hippocampus.** *Neurology* 1993;43:589–594
13. Thatcher NM, Prior MJW, Morris PG, Bachelard HS. **Magnetic resonance spectroscopy studies on changes in cerebral calcium and zinc and energy state caused by excitotoxic amino acids.** *J Neurochem* 1999;72:2471–2478
14. Kreis R. **Quantitative localized 1H MR spectroscopy for clinical use.** *J Prog Nucl Magn Reson Spectroscopy* 1997;31:155–195
15. Birken DL, Olendorf WH. **N-acetyl-L-aspartic acid: a literature review of a compound prominent in ^{1}H-NMR spectroscopic studies of brain.** *Neurosci Biobehav Rev* 1989;13:23–31
16. von Economo CV, Koskinas GN. **Übersichtstabellen der wichtigsten areae.** In: *Die Cytoarchitektonik der Hirnrinde des erwachsenen Menschen.* Berlin: Spinger; 1925;794–801
17. Urenjak J, Williams SR, Gadian DG, Noble M. **Proton nuclear magnetic resonance spectroscopy unambiguously identifies different neural cell types.** *J Neurosci* 1993;13:981–989
18. Ross BD. Blüml S. **New aspects of brain physiology.** *NMR Biomed* 1996;9:279–296
19. Brand A, Richter-Landsberg C, Leibfritz D. **Multinuclear NMR studies on the energy metabolism of glial and neuronal cells.** *Dev Neurosci* 1993;15:289–298
20. Norenberg MD. **Distribution of glutamine synthetase in the rat central nervous system.** *J Histochem Cytochem* 1979;27:756–762
21. Derouiche A, Frotscher M. **Astroglial processes around identified glutamatergic synapses contain glutamine synthetase: evidence for transmitter degradation.** *Brain Res* 1991;552:346–350
22. Schousboe A, Westergaard N, Waagepetersen HS, Larsson OM, Bakken IJ, Sonnewald U. **Trafficking between glia and neurons of TCA cycle intermediates and related metabolites.** *Glia* 1997; 21:99–105
23. Patel AJ, Weir MD, Hunt A, Tahourdin CS, Thomas DG. **Distribution of glutamine synthetase and glial fibrillary acidic protein and correlation of glutamine synthetase with glutamate decarboxylase in different regions of the rat central nervous system.** *Brain Res* 1985;331:1–9
24. Ernsberger P, Iacovitti L, Reis DJ. **Astrocytes cultured from specific brain regions differ in their expression of adrenergic binding sites.** *Brain Res* 1990;517:202–208
25. Kreis R, Ernst T, Ross BD. **Development of the human brain: in vivo quantification of metabolite and water content with proton magnetic resonance spectroscopy.** *Magn Reson Med* 1993;30:424–437